

MASS SPECTRA OF CERTAIN SOLID SUBSTANCES AND  
THEIR INTERPRETATION

M.S.Chupakhin and G.G.Glavin

FACILITY FORM NO.	N 65-19704	
	(ACCESSION NUMBER)	(THRU)
	15	1
	(PAGES)	(CODE)
		26
	(NASA CR OR TMX OR AD NUMBER)	(CATEGORY)

Translation of "Mass-spektry nekotorykh tverdykh  
veshchestv i ikh interpretatsiya".  
Zhurnal Analiticheskoy Khimii, Vol.19,  
No.7, pp.821-9, 1964.

GPO PRICE \$ \_\_\_\_\_

OTS PRICE(S) \$ \_\_\_\_\_

Hard copy (HC) \$1.00

Microfiche (MF) \$0.50

NATIONAL AERONAUTICS AND SPACE ADMINISTRATION  
WASHINGTON

MARCH 1965

MASS SPECTRA OF CERTAIN SOLID SUBSTANCES AND  
THEIR INTERPRETATION

\*/821

M.S.Chupakhin and G.G.Glavin

Vernadskiy Institute of Geochemistry and Analytical Chemistry,  
USSR Academy of Sciences; State Research and Planning  
Institute for the Rare Metals Industry, Moscow

19704

Experimental results obtained for the mass spectra of numerous solid substances, with a double-focusing mass spectrograph using a spark ion source, are given. Three mechanisms of the ion formation in the spark source are described (ionization by cathode sputtering, thermionic emission, ionization by electron and ion collisions). The lines of atomic and molecular oxygen in the mass spectra are used for analyzing alloyed and unalloyed specimens of graphite, silicon, germanium, boron, arsenic, etc. Tabulated data on the results are given.

The mass spectra of solid substances taken on a double-focusing spectrograph with a spark ion source are in many ways interesting and different from spectra taken with other types of ion sources. The simultaneous recording of almost the entire spectrum ( $m/e = 6 - 250$ ) on the photographic plate in a single experiment yields extensive data on the test sample and gives its elementary composition with a sensitivity of  $10^{-5} - 10^{-7}$  at.% (Bibl.1).

A spark source of ions forms singly-charged ions of the isotopes of both the base material and the impurities, multiply-charged ions mainly of the base

---

\* Numbers in the margin indicate pagination in the original foreign text.

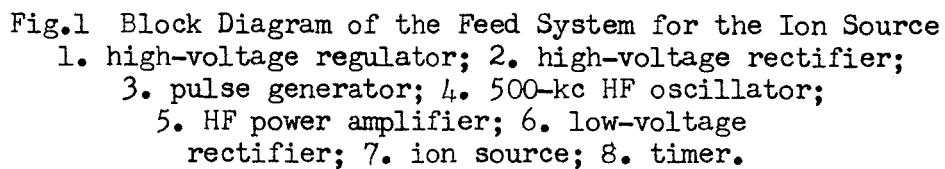
(and also of the impurities if their concentrations are sufficiently high), polyatomic complexes and supercharged ions. The secondary formations, consisting of polyatomic masses and various oxygen complexes, in some cases mask the masses of the impurity elements and make it difficult to identify them in the analytical samples. For example, in analyzing a Fe-Co-Ni alloy, the diatomic, triatomic, and tetraatomic ions of these elements make it difficult or impossible to register about 25 impurity elements with isotopes of the same mass numbers. This disadvantage, however, is compensated by the useful application of polyatomic and multiply-charged ions for analytical purposes. It has been shown (Bibl.2, 3) that the concentration of the polyatomic complexes registered in the analysis of graphite, and especially in that of silicon, vary widely, depending on the state and structure of these substances. The method of mass spectrometry, using a spark ion source and photographic recording, can determine not only the impurities uniformly distributed through a sample but also the impurities that have contaminated the surface during preparation of the electrodes for analysis (Bibl.1).

Before discussing the new experimental data obtained for a number of substances, let us consider the mechanisms of ionization in the spark ion source of a mass spectrometer.

Figure 1 is a block diagram of the feed system of a spark ion source.

The spark vacuum discharge in the ion source is due to a modulated voltage of high frequency, of the order of 500 kc. The pulse frequency may be varied from 10 to 3000 pps, and the pulse duration  $\tau$ , from 25 to 200  $\mu$ sec. The pulse voltage is regulated between 0 and 100 kv. An accelerating DC voltage of 20 kv is applied between the electrodes of the specimen (a, b) and the first slit ( $S_1$ ) of the ion source, on the one hand, and the second grounded slit ( $S_2$ ), on

The second half of the slit ( $S_2$ ) is used for blocking the ion beam by 4822 application of a potential of +1600 v across a time gate. The blocking potential is turned on automatically depending on the position of the commutator.



This device is used to adjust the ion dosage when selecting the exposure.

The high-frequency pulse discharge in the vacuum is made to take place in a small volume by closely approaching the electrodes a and b, made of the material to be tested which is either a nonconductor or a poor conductor.

There is at present no general consensus on the very complex process of spark ionization. The experimental data permit a provisional delineation of several simultaneous mechanisms of excitation of ions. The collision of ions, along their path in the analyzer, with residual molecules and atoms will produce continuous background bands, lines, and adjoining bands on the photographic plate.

Let us consider the ionization mechanism in the spark ion source during analysis of solid substances in the mass spectrometer:

1. Ionization by cathode sputtering ( $I_1$ ).
2. Thermionic emission of elements with low ionization potentials ( $I_2$ ).
3. Ionization by electron and ion collision: a) ions of the residual gases ( $I_3$ ); b) ionized molecules and fragments of the hydrocarbons entering the ion source from the diffusion pump ( $I_4$ ); c) ions of the material of the screen and slits ( $S_1$  and  $S_2$ ), as well as the atoms of the "memory" of the preceding specimen ( $I_5$ ).

Thus the total ion current of the source is composed of the sum of the currents:

$$I_{\text{total}} \approx I_1 + I_2 + I_3 + I_4 + I_5. \quad (1)$$

In most cases the ions of the same element are formed in several different ways and, after separation by the magnetic field, are recorded on the photographic plate in accordance with their mass and charge. /823

Cathode sputtering, formation of ionized particles during such sputtering, and the subsequent ionization of the sputtered material in the spark gap are the most important source of ionization in the spark ion source. Cathode sputtering is the primary cause of ionization in the spark source. Cathode sputtering is the result of ion collisions and vaporization (Bibl. 4 - 6). The



Fig.2 Mass Spectra of Graphite, Silicon Carbide and Silicon

energy of the ions is imparted to a rather large number of ions of the test material, accompanied by simultaneous strong local heating on a very small area of its surface. Before the heat is redistributed through the interior, there is a hydrodynamic ejection of the vaporized substance in the form of streamers (Bibl.7) consisting of ions and neutral particles, a certain number of which are later ionized in the spark channel. However, the mean temperature of the electrode surface remains relatively low, hardly exceeding 500-700°K.

If cathode sputtering is considered as an elastic collision between a high-energy ion and the lattice atoms of the specimen, then - in first approximation - the relation between the coefficient of cathode sputtering and the mass may be expressed in the form of

$$N = \sqrt{\frac{eE}{E_s}} \cdot \sigma, \quad (2)$$

where  $\epsilon = \frac{2M_1 M_2}{(M_1 + M_2)^2}$ ;  $M_1$  and  $M_2$  are the respective masses of the bombarding and sputtered atoms;  $\sigma$  represents the

processes connected with the secondary effects of the interaction in the lattice of the specimen;  $E_a$  is the lattice binding energy; and  $E$  is the energy of the bombarding ion.

Experiments have shown that a spark discharge detaches not only individual atoms from the electrodes but also polyatomic fragments of the lattice of the test sample whose ions also appear in the spectrum (Fig.2).

Masses up to  $C^{20}$  are observed in the graphite spectra of Fig.2 ( $C^{19}$  and  $C^{20}$  are not shown on the photograph), and up to  $Si^7$  for silicon. Evidence that these polyatomic molecules are not formed from the vapors of graphite and silicon is provided by the mass spectrum of silicon carbide, which does not show the characteristic spectra of its constituents. As will be seen from Fig.3, the yields of  $C^2$ ,  $C^3$ ,  $C^4$ , etc., and of  $Si^2$ ,  $Si^3$ ,  $Si^4$ , etc. as well as those of the polyatomic molecules of silicon carbide, follow a definite sequence for the even and odd components, suggesting that the formation of complexes of the test sample during the spark discharge is due to the breakdown of the structure at its weakest bonds. We have already discussed the formation of polyatomic formations of graphite and silicon in greater detail (Bibl.2, 3).

The concentrations of multiply-charged ions of the test substances decline by an average factor of 6 - 10 as the degree of ionization increases. This is only partially true, however. In pure unalloyed semiconductor silicon, the ratio of  $Si^+/Si^{++}$  is in fact close to 10, while it is considerably higher in silicon alloyed with arsenic or boron. The same phenomenon is also noted in the case of germanium (Table 1).

With increasing concentration of the alloying impurity arsenic or boron in silicon and germanium, the ratio of  $M^+/M^{++}$ , i.e.,  $Si^+/Si^{++}$  and  $Ge^+/Ge^{++}$  also

increases, but then again decreases as soon as the arsenic content of silicon rises above  $1 \times 10^{20} \text{ cm}^{-3}$  (see Table 1). For instance, in the specimen No.6, which shows dislocations and a cellular structure, the concentrations of /824  $\text{Si}^+$  and  $\text{Si}^{++}$  are practically the same. The  $\text{Si}^+/\text{Si}^{++}$  is particularly high for

TABLE 1  
RATIO OF SINGLY-CHARGED TO DOUBLY-CHARGED IONS OF MONOCRYSTALLINE  
SILICON AND GERMANIUM IN UNALLOYED AND ALLOYED SPECIMENS

Specimen No.	Material	Alloying Addition $\text{cm}^{-3}$	$\text{M}^+/\text{M}^{++}$ Ratio	Remarks
1	Si	-	7	Dislocations
2	"	-	10	" "
3	"	As $2.7 \times 10^{17}$	20	No dislocations
4	"	" $1 \times 10^{19}$	40	" "
5	"	" $1 \times 10^{20}$	25	" "
6	"	" $3.5 \times 10^{20}$	2	Dislocations
7	"	B $1.08 \times 10^{18}$	50	No dislocations
8	"	" $5 \times 10^{19}$	45	" "
9	Ge	-	12	-
10	"	As $3.4 \times 10^{19}$	25	No dislocations

silicon alloyed with boron (specimens Nos. 7 and 8). It is well known that no dislocations are observed in silicon with an arsenic or boron concentration in the range from  $1 \times 10^{17}$  to  $1 \times 10^{19} \text{ cm}^{-3}$ , while unalloyed silicon or silicon with more than  $10^{19} \text{ cm}^{-3}$  of arsenic shows dislocations. The data in Table 1 indicate a correlation between the ratio of singly- and doubly-charged ions and the presence of dislocations in silicon and germanium.

It was of great interest to compare the ratio of singly- to doubly-charged ions of silicon with the ratios of ions of the same charge in porous substances. For this purpose, we studied ferrite specimens prepared by the same method from the same starting materials, but with different magnetic permeability; one /825 of them was graded "acceptable" and the other "reject".



It is well known that the quality of ferrite articles is judged by their porosity in addition to many other factors (Bibl.8). The  $\text{Fe}^+/\text{Fe}^{++}$  ratio for an "acceptable" article was found to be 50, that for a "reject" about 350.

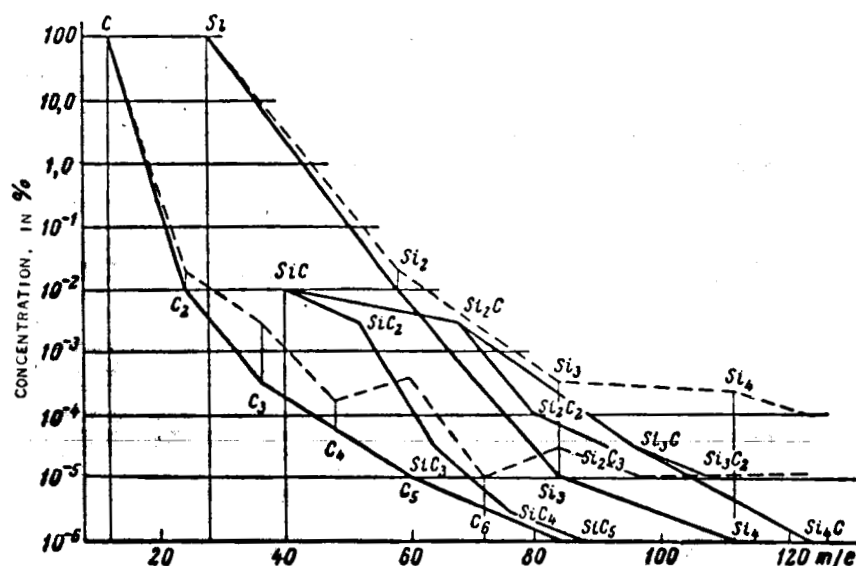


Fig.3 Concentration of Polyatomic Formations in Graphite, Silicon Carbide and Silicon  
 - - - Yield of polyatomic complexes from specimens of silicon and graphite

Evidently the high  $\text{Fe}^+/\text{Fe}^{++}$  ratio in the "reject" can be explained by the fact that its porosity is greater than that of the "acceptable" article. The concentration of ions with a charge higher than triple in no way correlates with any properties of the substance, and their yield varies practically everywhere in the same way, by a factor of the order of 6 to 8 for each degree of ionization. Still another conclusion can be drawn from these data: In the spark ion source, the singly- and doubly-charged ions and, to some extent, also the triply-charged ions, are formed by the same process as are the polyatomic configurations whereas the higher-charged ions are formed by another. The latter are apparently formed in the spark channel, where the temperature of the plasma

reaches some 40,000°K (Bibl.7). At such a temperature the polyatomic complexes naturally dissociate into atoms, and therefore even doubly-charged masses of polyatomic molecules, such as  $\text{Si}_3^{++}$  etc., are no longer observed in the spectrum.

The second method of ion formation in the spark source is by thermionic emission for elements of low ionization potential. This phenomenon is particularly well observed for Li, Na, K, and Ca.

The cause of the thermion formation is the heating of the electrode surfaces near the discharge. Since the degree of ionization of atoms in thermionic emission is considerably greater than that of ionization in a spark, the concentration of these elements is higher than the content in the sample, as recorded on the photographic plate. It is true that this is not invariably observed. In many cases, the concentration of the elements with a low ionization potential coincides with their true level in the specimen, but in this case the ratio of singly- to doubly-charged ions of these elements is the same as for the other impurities. This difference can be explained by assuming that in the one case the elements were on the surface, while in the other they were uniformly distributed throughout the specimen.

Thus, in determining the concentration of elements with a low ionization potential, we first compare the ratios of singly- to doubly-charged ions, and if these ratios are beyond the allowable limits, then the sodium is determined from the  $\text{Na}^{++}$ , the potassium from the  $\text{K}^{++}$ , the lithium from the  $\text{Li}^{++}$ , and the calcium from the  $\text{Ca}^{++}$ . The same also holds for Ba, Cs, Rb, Sr, etc., although in practice this is almost never necessary for these elements.

Ions of the oxygen and nitrogen contained in the materials to be tested are also formed in the spark source. Ions of these elements, however, may be

formed by ionization of the atoms and molecules of the residual gas in the source. Consequently, it is difficult to determine the contents of these elements in the samples from the masses of O and O<sub>2</sub>, N and N<sub>2</sub>. Further than that, the mass of N<sub>2</sub> ( $m/e = 28$ ) coincides with the mass of silicon, and N<sup>++</sup> with Li<sup>7+</sup>. The difficulty of determining these elements is still further complicated by the fact that the residual pressure in the region of the ion source is not reproducible from experiment to experiment.

As already mentioned, the molecules and molecule fragments of hydrocarbons whose vapors had leaked into the ion source from the diffusion pumps are also ionized in that source. The ions of such molecules and fragments are mostly recorded on the left side of the spectrum, up to mass 40. Overlapping of these lines by the lines of the isotopes of Mg, Al, Si, P, K, and Ca was most often observed. For example, the C<sub>2</sub> line was superposed on mass 40 (Mg), the C<sub>2</sub>H<sub>3</sub> line on the Al line, the C<sub>2</sub>H<sub>4</sub> line on the Si line, etc. Owing to the insufficient resolution of the instrument, these masses coincide with the impurity masses of the specimen, complicating their registration. To avoid wrong conclusions as to the concentration of such elements in the specimens, any /826 interpretation of the mass spectra must allow for the relative abundance of the isotopes of the impurity elements and use a comparison of the concentrations of singly- and doubly-charged ions. If the abundance of the isotopes of a given element, as shown on the photographic plate, does not agree with the abundance given in the Tables, then that particular impurity is determined from the doubly-charged ions, if they are not superposed by other masses. The sensitivity of the determination will of course be lower than on recording on the basis of the principal masses. Finally, the plate also registers lines from the "memory" of the preceding specimen, and from the tantalum of the

holder.

To eliminate this storage effect, the traces of the preceding substance are carefully removed before making an analysis, and a blank is also run. The tantalum in the instrument (used in the shields and in parts of the ion source) does not form doubly-charged ions, although singly-charged ions appear on collision of the specimen ions with the material of the specimen holder. Impurity tantalum forms both singly- and doubly-charged ions and can thus be distinguished from the instrument tantalum. Still another group of lines appeared on the photographic plate in each of our experiments. These lines correspond to the masses of the overcharged multi-charge ions. Their intensity is greater, the poorer the vacuum of the system. Such overcharging takes place in the electrostatic and magnetic analyzers, and produces solid background bands on the plate. This background always shifts in the direction of the light masses. Overcharged ions that form lines and narrow bands on the photographic plate are also formed in the gap between the electrostatic and magnetic analyzers. The mechanism of overcharging can be demonstrated on the example of silicon:



where M is a molecule or atom of the residual gas in the analyzer. After overcharging, the silicon ion occupies a different site, not corresponding to its mass, on the photographic plate. The location of the overcharged ion on the plate is determined by the formula:

$$m' = m \cdot \frac{q_1}{q_2} (1 - k), \quad (5)$$

where  $m'$  is the position occupied by the ion on the plate after its overcharg-

ing;  $m$  is the mass of the isotope of this element;  $q_1$  is the charge of the ion before overcharging;  $q_2$  its charge after overcharging; and  $k$  the loss of energy by the ion on collision with residual molecules or atoms of the gas. For instance,  $\text{Si}^{28++}$ , on collision with the particle  $M$ , captures an electron and therefore occupies the position  $m' = 56 (1 - k)$  on the plate. When the vacuum in the analyzer decreases, a sensible concentration of overcharged  $\text{Si}^{28++}$  ions appears in the analyzer. Their position on the plate is determined by eq.(5) if the values  $m = 28$ ,  $q_1 = 3$ ,  $q_2^2 = 4$  are substituted in it. Then, we have  $m' = 21 (1 - k)$ . The overcharged ions are recorded somewhat to the left of the main mass in the form of bands, as indicated in Fig.2 [the line next to  $\text{Si}_2$  ( $m/e = 56$ )].

The future use of the lines of atomic and molecular oxygen for analytical purposes will probably be possible. To each of the substances given in Table 2 there corresponds a yield of atomic and molecular oxygen that differs from all others. In graphite, for instance, oxygen is registered only in high-impurity specimens, and is almost never observed in a spectrally pure electrode /827 (specimen No.1). A low oxygen content was found in specimen No.5, in which only small amounts of other impurities were found.

It is likewise characteristic that only atomic oxygen should have been noted, while both atomic and molecular oxygen were found in germanium.

The oxygen compounds of the elements being determined are found rather frequently in the analysis of titanium, zirconium and other materials, and may be utilized, though as yet only qualitatively, for estimating the oxygen content. Further experiments will be necessary on specimens with known gas content, determined by the method of vacuum melting or isotope dilution.

In this connection, the data on the analysis of ferrites, in which oxygen

compounds of iron are recorded, seem of interest. For this purpose, we took two articles prepared in the same manner from the same materials, but of different direct and inverse inductance loss ( $L_{dir}$  and  $L_{inv}$ ). Mass spectrometry

TABLE 2

CONTENTS OF ATOMIC AND MOLECULAR COMPONENTS OF OXYGEN ON MASS  
SPECTROMETRIC ANALYSIS OF SEVERAL SOLID SUBSTANCES

Specimen No.	Material	$O^+$ , at. %	$O_2^+$ , at. %	Remarks
1	Graphite	-	-	Spectrally pure
2	"	$1 \times 10^{-3}$	$1 \times 10^{-3}$	High ash
3	"	$1 \times 10^{-3}$	$3 \times 10^{-3}$	
4	"	$1 \times 10^{-2}$	$3 \times 10^{-2}$	
5	"	$3 \times 10^{-4}$	-	Pure
6	Si + $2.5 \times 10^{19} \text{ cm}^{-3} \text{ B}$	$3 \times 10^{-1}$	-	
7	Si + $1 \times 10^{20} \text{ cm}^{-3} \text{ As}$	$6 \times 10^{-1}$	-	
8	Si	$4 \times 10^{-1}$	-	Unalloyed
9	Ge	$2 \times 10^{-3}$	$2 \times 10^{-5}$	"
10	Ge + $3.4 \times 10^{19} \text{ cm}^{-3} \text{ As}$	$6 \times 10^{-2}$	$2 \times 10^{-3}$	
11	Nb	2	$1 \times 10^{-1}$	
12	Sikhote-Ala meteorite	$2 \times 10^{-1}$	$2 \times 10^{-3}$	

showed the same ratio of singly- to doubly-charged ions of iron (having a value of about 10). Thus, there was no difference in porosity, as with the previous specimens. The only difference found was in the  $\text{FeO}^+$  content, which was 12.5 times as great in the "rejected" article as in the "accepted" one. Divalent iron is known to have an adverse effect on the ferrite quality. Our data are not inconsistent with this fact.

In conclusion, we wish to thank A.P.Vinogradov, N.P.Sazhin, I.P.Alimarin and D.I.Ryabchikov for their attention to, and interest in, our investigations. We express our sincere gratitude to V.I.Fistul' for participating in the discussion of the results and to L.G.Abeleva for helping in the experiments and

in the arrangement of this work.

# BIBLIOGRAPHY

1. Chupakhin, M.S. and Glavin, G.G.: Zhurn. analit. khimii, Vol.18, p.618, 1963.
2. Chupakhin, M.S., Glavin, G.G., and Fistul', V.I.: Dokl. AN SSSR, Vol.150, p.1059, 1963.
3. Chupakhin, M.S., Glavin, G.G., and Duyev, L.T.: Zhurn. tekhn. fiz., Vol.33, p.1132, 1963.
4. Hippel, A.: Ann. Phys., Vol.81, p.1043, 1926.
5. Hippel, A. and Elechsmidt, E.: Ibid., Vol.86, p.1006, 1928.
6. Townes, Ch.H.: Phys. Rev., Vol.65, p.319, 1944.
7. Sukhodreyev, N.K.: Acta chim. Acad. Sci. Hung., Vol.30, p.285, 1963.
8. Smit, Ya. and Veyn, Kh. [J.Smith and H.Wein]: Ferrites (Ferrity). Foreign Literature Press, Moscow, p.360, 1963.

Received July 27, 1963.